ORIGINAL ARTICLE

Plant, Cell &
Environment

PCE WILEY

Field-work reveals a novel function for MAX2 in a native tobacco's high-light adaptions

Suhua Li[1,2] | Gundega Baldwin[2] | Caiqiong Yang[2] | Ruirui Lu[1] | Shuaishuai Meng[1] | Jianbei Huang[3] | Ming Wang[2,4] | Ian T. Baldwin[2]

[1]Shenzhen Branch, Guangdong Laboratory of Lingnan Modern Agriculture, Key Laboratory of Synthetic Biology, Ministry of Agriculture and Rural Affairs, Agricultural Genomics Institute at Shenzhen, Chinese Academy of Agricultural Sciences, Shenzhen, China

[2]Department of Molecular Ecology, Max Planck Institute for Chemical Ecology, Jena, Germany

[3]Department of Biogeochemical Processes, Max Planck Institute for Biogeochemistry, Jena, Germany

[4]Department of Plant Pathology, Nanjing Agricultural University, Nanjing, China

Correspondence
Ian T. Baldwin and Ming Wang, Department of Molecular Ecology, Max Planck Institute for Chemical Ecology, Jena, Germany.
Email: baldwin@ice.mpg.de and mwang@njau.edu.cn

Abstract

Laboratory studies have revealed that strigolatone (SL) and karrikin (KAR) signalling mediate responses to abiotic and biotic stresses, and reshape branching architecture that could increase reproductive performance and crop yields. To understand the ecological function of SL and KAR signalling, transgenic lines of wild tobacco *Nicotiana attenuata*, silenced in SL/KAR biosynthesis/signalling were grown in the glasshouse and in two field plots in the Great Basin Desert in Utah over four field seasons. Of the lines silenced in SL and KAR signalling components (irMAX2, irD14, irKAI2 and irD14 × irKAI2 plants), which exhibited the expected increases in shoot branching, only irMAX2 plants showed a strong leaf-bleaching phenotype when grown in the field. In the field, irMAX2 plants had lower sugar and higher leaf amino acid contents, lower lifetime fitness and were more susceptible to herbivore attack compared to wild-type plants. These irMAX2 phenotypes were not observed in glasshouse-grown plants. Transcriptomic analysis revealed dramatic responses to high-light intensity in irMAX2 leaves in the field: lutein contents decreased, and transcriptional responses to high-intensity light, singlet oxygen and hydrogen peroxide increased. PAR and UV-B manipulations in the field revealed that the irMAX2 bleaching phenotype is reversed by decreasing PAR, but not UV-B fluence. We propose that *NaMAX2* functions in high-light adaptation and fitness optimisation by regulating high-light responses independently of its roles in the SL and KAR signalling pathways. The work provides another example of the value of studying the function of genes in the complex environments in which plants evolved, namely nature.

KEYWORDS
field-based phenotyping, *Nicotiana attenuata*

1 | INTRODUCTION

Plants in nature face complex environments and phytohormones play central roles in coordinating a plant's physiological responses to complex suites of environmental stresses. Desert environments are commonly characterised by intense sunlight with high fluences of photosynthetically active radiation (PAR) and ultraviolet (UV-B) radiation, low water- and nutrient-availability, extreme heat, wind- and sand-storms, in addition to intense herbivore pressures. *Nicotiana attenuata* is a tobacco, native to the Great Basin Desert of the western USA, and hence evolved with these abiotic and biotic stresses. Planting *N. attenuata* plants silenced in the biosynthesis and perception of various phytohormones has proved to be a valuable means of evaluating their function in adapting physiology to environmental stresses. For instance, previous work with this species has revealed that jasmonate (JA) hormones are critical modulators of herbivore defence in the field: for example, *N. attenuata* plants deficient in the accumulation and perception of JA are frequently heavily attacked by *Empoasca* leafhoppers (Kallenbach et al., 2012).

Strigolactones (SLs) are carotenoid-derived hormones that regulate plant architecture by inhibiting shoot branching (Gomez-Roldan et al., 2008; Umehara et al., 2008). They also function as rhizosphere signals between host plants and parasitic plants as well as symbiotic fungi (Akiyama et al., 2005; Cook et al., 1966). DWARF 14 (D14), an α/β-fold hydrolase, is the receptor of SLs (Nakamura et al., 2013; Waters et al., 2012a; Yao et al., 2016). Karrikins (KARs) are a group of smoke-derived chemicals that stimulate seed germination after fires. The receptor of KARs, KARRIKIN INSENSITIVE 2 (KAI2), is a paralogue of D14 (Waters et al., 2012b). Signalling triggered by SLs and KARs both requires the same coreceptor, MORE AXILLARY GROWTH2 (MAX2), a leucine-rich-repeat F-box protein (Nelson et al., 2011). *max2* mutants in various plant species, including Arabidopsis and rice (in which they are called *dwarf 3*) are insensitive to both SL and KAR signals (Nelson et al., 2011; Smith & Li, 2014; Zhao et al., 2014).

SL-biosynthetic and -signalling mutants have been generated in *Arabidopsis*, rice and petunia, and all exhibit increased branching (Gomez-Roldan et al., 2008; Hamiaux et al., 2012; Ishikawa et al., 2005; Umehara et al., 2008). In addition, the SL pathway is known to regulate additional traits that influence yield, such as the kernel weight in maize and panicle development in rice (Guan et al., 2022; Wang et al., 2020). SLs and KARs also play central roles in defence against biotic attackers, such as against the larvae of stem-boring weevils, *Trichobarus mucorea* (Li et al., 2020), as well as against nematodes (Lahari et al., 2019; Xu et al., 2019). Both SL and KAR signals improve survival under drought and salt stress (Ha et al., 2014; Li et al., 2017) and recent studies with tomato, revealed a role for SLs in heat and cold tolerance (Chi et al., 2021). Together, these results suggest that SL and KAR-signalling could be promising targets to increase crop yields. However, the majority of these studies have been performed in glasshouse or laboratory environments, and the roles played by SL- and KAR-signalling in natural environments remains unresolved.

Plants are commonly grown in glasshouses or chambers to infer development and performance in the field, but these environments differ in important ways. For example, the glasshouse light environment is commonly only a fraction of the PAR intensity of full sunlight and often lacking UV-B entirely (Poorter et al., 2016; Schuman & Baldwin, 2018). Plants growing in the Utah desert, for example, are regularly exposed to 2000 μmol/m^2/s of PAR and several hundreds μmol/m^2/s of UV-B, conditions which are challenging to replicate in controlled environments. Exposure to light levels that exceeds photosynthetic capacity can result in photo-oxidative stress and chlorophyll damage (Li et al., 2009a), and plants have evolved photoprotective measures that minimise the damage caused by excess light, such as photorespiration, nonphotochemical quenching (NPQ), and the accumulation of superoxide dismutase (SOD), and antioxidants, such as carotenoids that prevent chlorophyll oxidation (Ramel et al., 2012; Sánchez-Moreiras & Reigosa, 2018). These biochemical responses to high-light stress are embedded in a suite of morphological and cellular responses that include leaf movement (Sofo et al., 2015), movement of chloroplasts within a cell (Kasahara et al., 2002; Sztatelman et al., 2010; Zurzycki, 2017) and changes in the molecular organisation of the thylakoid membranes (Janik et al., 2013). Whether SL- and KAR-signalling plays a role in these excess-light responses remains unknown.

When *N. attenuata* plants, silenced in SL- and KAR-signalling, are grown in the glasshouse, their reproductive performance is greater than that of isogenic empty vector (EV) transformed plants, due to increased branching, total biomass, floral and seed capsule production. Moreover, their herbivore resistance was unaltered. However, when planted into the plant's native habitat, the Great Basin Desert of Utah, *MAX2* was identified as a key gene regulating high-light responses. Silencing *MAX2*, but not *D14* and *KAI2*, either alone or together, resulted in leaf-bleaching, with decreased chlorophyll contents, photosynthetic abilities, fitness and herbivore resistance. The bleaching phenotype of irMAX2 plants was recovered by PAR, but not UV-B shading in the field. The mechanisms by which *MAX2* regulate excess-light-triggered responses was examined with transcriptomic analyses and measures of sugars, amino acids, antioxidants and peroxide levels. From these results, we infer that *MAX2* enhances plant fitness in nature via the regulation of high-light responses and antioxidant accumulations, independently of SL- and KAR-signalling.

2 | RESULTS

2.1 | Silencing *NaMAX2* enhances fitness of glasshouse-grown plants

Independent lines of isogenic *N. attenuata*, silenced in *NaMAX2*, *NaD14* and *NaKAI2* expression by RNA interference (RNAi) were compared with plants transformed with an EV transformation construct, as a control. As expected, both lines of irD14 and irMAX2 plants, but not irKAI2 plants, produced more primary branches and were of shorter overall stature (Figure 1a, Supporting Information: Figure S1a). irMAX2 plants were less sensitive than EV plants regarding the inhibition of hypocotyl elongation (Li et al., 2020) in
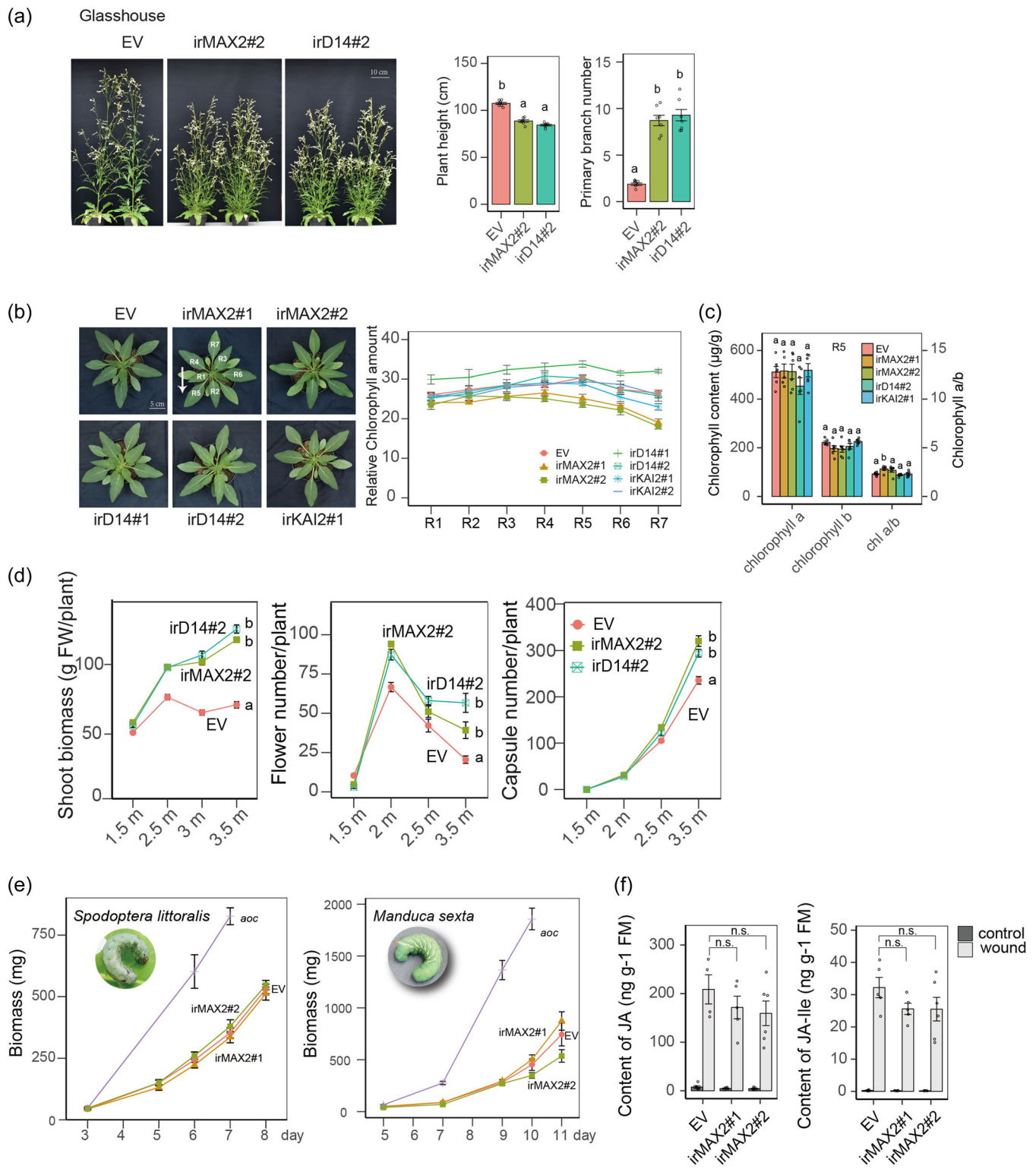
FIGURE 1 *MAX2* silencing in glasshouse-grown *Nicotiana attenuata* plants enhances growth and fitness without compromising herbivore resistance. (a) Plant height and primary branch numbers of 3.5-month-old EV, irMAX2#2 and irD14#2 plants grown in the glasshouse (*n* = 8). (b, c) Rosette-stage phenotypes and relative chlorophyll amounts (*n* = 8) (b), contents of chlorophyll a, b and chl a/b ratio (*n* = 6) (c) of 30-day-old indicated plants. (d) Shoot biomass, flower numbers, capsule numbers of EV, irMAX2#2 and irD14#2 plants at indicated months (*n* = 8–12). Data collected at 3.5 months were used for statistical analysis. (e) Larval mass of the generalist (*Spodoptera littoralis*) and specialist (*Manduca sexta*) Lepidopteran herbivores feeding on EV, irMAX2#1, irMAX2#2 and defenceless (irAOC) plants at the indicated days (*n* = 16–28). (f) Levels of JA and JA-Ile in EV, irMAX2#1 and irMAX2#2 leaves without (control) or with a leaf-lamina puncture-wound treatment after 1 h (*n* = 6). Statistical analyses were performed using Turkey's multiple comparisons test (*p* < 0.05) (a, c, d) or two-tailed *t*-test (n.s. no significant difference) (f) (all values are means ± SE).

response to GR24 treatments, and the sequence used in the RNAi constructs had no off-target in the *N. attenuata* exome with an n-mer size of 21 bp (Supporting Information: Figure S1b). These results revealed that *N. attenuata* irMAX2 plants exhibited the same growth and branching phenotypes as other irMAX2 mutants in other plant species, such as *Arabidopsis* and rice (Gomez-Roldan et al., 2008; Ishikawa et al., 2005; Li et al., 2016; Umehara et al., 2008).

When grown in the glasshouse, irMAX2, irD14 and irKAI2 plants did not differ in their chlorophyll contents, including chlorophyll a and b and the ratio of a/b in rosette leaves, compared with EV plants (Figure 1b,c). After 2 months of growth, irD14 and irMAX2 plants attained significantly larger shoot biomass and flower numbers, and after 2.5 months of growth, greater capsule numbers (Figure 1d). Feeding assays with the larvae of the generalist, *Spodoptera littoralis*, and the specialist, *Manduca sexta*, herbivores revealed that both species performed similarly when feeding on EV and irMAX2 plants, while both species gained significantly more biomass when feeding on the defenceless irAOC plants, silenced in the expression of the JA-biosynthetic gene, *ALLENE OXIDE CYCLASE* (Figure 1e). Moreover, the wound-elicited bursts of JA and JA-Ile levels in irMAX2 leaves at 1 h did not differ significantly from those of EV leaves (Figure 1f). From these results, we infer that silencing *MAX2* expression increases biomass and seed production, without influencing herbivore resistance, suggesting that silencing *MAX2* might be an efficient strategy to improve plant fitness.

2.2 | In the field, silencing *NaMAX2* results in leaf-bleaching and impairs plant fitness

To evaluate if these results from glasshouse-grown plants could be extended to growth in the field, we planted EV, irMAX2, irD14 and irKAI2 plants in their native habitat, the Great Basin Desert in Utah, USA, in two field plots (Lytle plot and Snow plot) over 4-years of field seasons (2018–2021) (Supporting Information: Figure S1c). As expected, in the 2018 and 2019 field seasons, irMAX2 plants were smaller and bushier, with larger numbers of primary branches, compared to initially size-match EV plants (Figure 2a, Supporting Information: Figure S1d). Surprisingly, three independent lines of irMAX2 plants consistently showed severe leaf-bleaching with significantly decreased chlorophyll a and b contents in leaves during four field seasons (Figure 2a,b,c, Supporting Information: Figure S1). irD14, irKAI2 and the crossed line of irD14 and irKAI2 (irD14 × irKAI2) plants did not show this bleaching (Figure 2a,b, Supporting Information: Figure S1e–g). As D14 and KAI2 are the receptors of SL- and KAR-signalling, respectively, these results suggesting that MAX2 regulates this bleaching phenotype in a SL- and KAR-signalling independent manner.

In the 2018 and 2019 field seasons, in contrast to glasshouse-grown plants, irMAX2 plants, but not irD14, irKAI2 or irD14 × irKAI2 plants, had decreased shoot biomass, flower and capsule numbers compared to EV plants (Figure 2d,e, Supporting Information: Figure S1h). In addition, in the field, the leaves of irMAX2 plants

were more heavily damaged by folivores (Figure 2f), and wound-induced JA bursts (JA, JA-Ile levels) were significantly lower in irMAX2 leaves than in EV leaves (Figure 2g). In contrast, in irD14, irKAI2, irD14 × irKAI2 leaves, these measures of herbivore resistance did not differ from those of EV plants (Figure 2f,g). From these results, we infer that silencing *MAX2* in field-grown *N. attenuata* plants results in leaf-bleaching, decreased plant fitness, and herbivore resistance, independent of SL- and KAR-signalling.

## 2.3 | In the field, silencing *NaMAX2* alters leaf primary metabolite levels

To compare the levels of nutrients in irMAX2 and irD14 leaves, we first analysed leaf starch and soluble sugar contents. Soluble sugars, including glucose, fructose and sucrose, did not differ in leaves of irMAX2 and irD14 glasshouse-grown plants (Figure 3a). However, in irMAX2 bleached leaves of field-grown plants, starch and soluble sugar levels were dramatically reduced (Figure 3b). Glasshouse-grown irMAX2, irD14 and EV plants contained similar levels of amino acids (Figure 3c). However, in field-grown plants, the total amino acid contents in irMAX2 leaves, but not in irD14 leaves, were two-fold higher than those of EV leaves, with some amino acids exceeding these increases, such as asparagine (11-fold), tryptophan (10-fold), arginine (seven-fold), isoleucine (seven-fold), valine (six-fold) and leucine (five-fold) (Figure 3d).

## 2.4 | Transcriptional responses in bleached irMAX2 leaves

To explore the reasons for irMAX2's bleaching, a microarray assay was conducted with EV, irMAX2, irKAI2 and irD14 leaves from the field. Multidimensional scaling (MDS) analysis clearly separated irMAX2 samples from EV, irKAI2 and irD14 samples (Figure 4a). Differentially expressed genes (DEGs) ($|\log_2 FC| \geq 1$, FDR ≤ 0.05) including 640 upregulated and 683 downregulated DEGs specifically altered in irMAX2 leaves were identified through Venn diagrams and are presented in heat-map displays (Figure 4b,c). These DEGs were further used to compute the enrichment of gene ontology (GO) terms, which revealed that upregulated genes were enriched in processes associated with responses to heat, light intensity and oxidative stress, while downregulated genes were enriched in responses to nutrient starvation (Figure 4d). These results identified heat and nutrient starvation as possible causes of the bleached phenotype of irMAX2 plants.

To evaluate if nutrient starvation was responsible for the bleaching of irMAX2 leaves, we measured macro- and micro-elements levels in the leaves of all transgenic plants. Most elements including carbon (C), potassium (K), iron (Fe) and magnesium (Mg) did not differ among the lines (Supporting Information: Figure S2a). While nitrogen (N) and phosphorus (P) were slightly increased in irMAX2 leaves (Supporting Information: Figure S2a), principal components analysis (PCA) of elements in irMAX2 plants showed
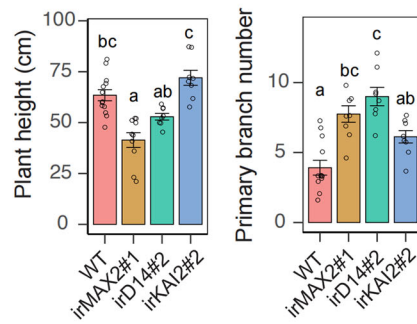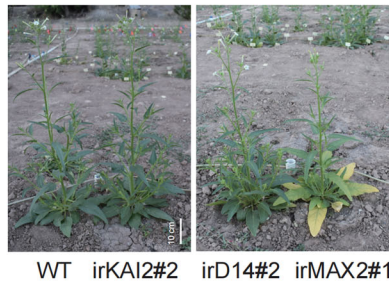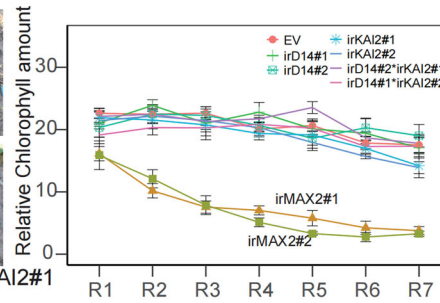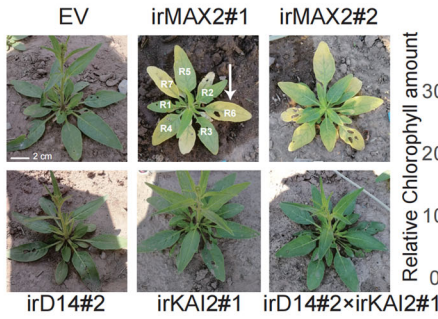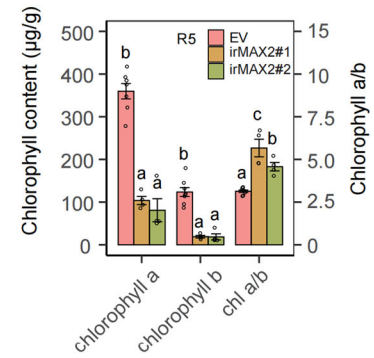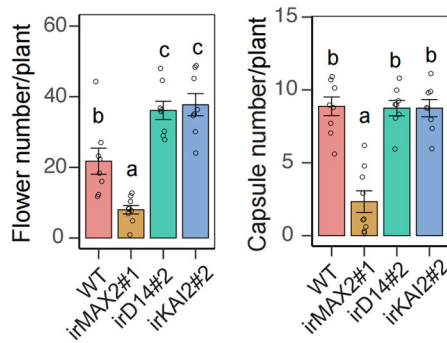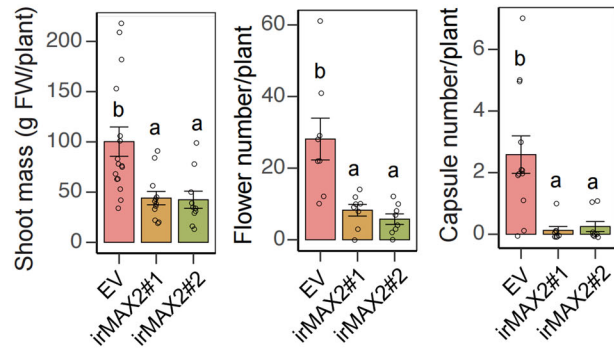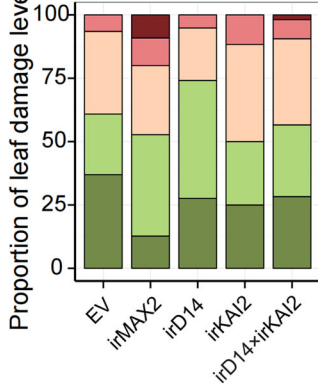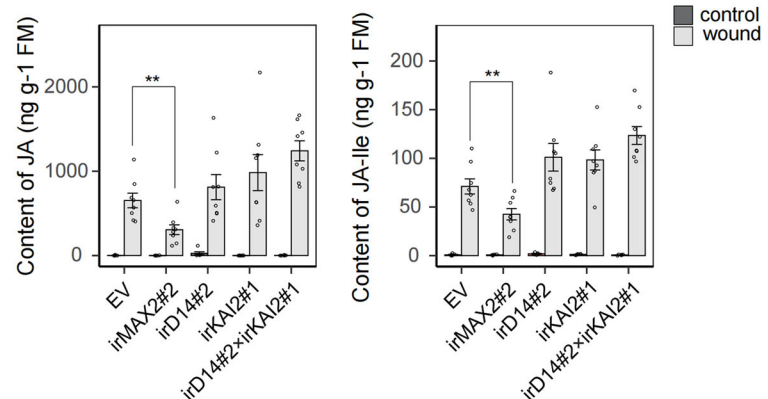
FIGURE 2 (See caption on next page).

no significant differences from those of all the other transgenic plants (Supporting Information: Figure S2b). From these results, we infer that nutrient deficiencies were not likely responsible for the bleaching of irMAX2 leaves.

As the GO term, responses to heat, was enriched in the upregulated DEGs of irMAX2 leaves, we examined the temperatures recorded by the meteorological station at the field station, which included a thermometer buried at a 20 cm depth in the centre of the rye field plot. Soil temperatures at night and daylight hours was consistently over 20°C, and attained 30°C at midday (Supporting Information: Figure S2c); during the 2021 field season a majority of midday soil temperature readings were over 20°C, and in July, most were over 30°C (Supporting Information: Figure S2d). Leaf temperatures of WT plants were over 30°C during 2019 field season (Supporting Information: Figure S2e) and approached 35°C already in May during the 2018 field season (Supporting Information: Figure S2f); no significant differences between WT and irMAX2 plants were observed (Supporting Information: Figure S2f). To evaluate if growth at high temperatures could result in leaf bleaching, we grew all transgenic lines in a growth chamber maintained at 35°C for 20 days (Supporting Information: Figure S2g). The leaves of irMAX2 plants did not bleach and their chlorophyll contents did not differ from those of EV plants (Supporting Information: Figure S2h), suggesting that heat alone was not responsible for irMAX2's bleaching in field-grown plants.

2.5 | PAR-shading in the field rescues the bleaching-phenotype and photosynthetic ability of irMAX2 plants

From the transcriptome data (Figure 4d), genes responsive to oxidative stresses and high-intensity light were upregulated in irMAX2 leaves. To evaluate if the high UV-B or PAR levels that characterise the desert light environment was responsible for the observed leaf-bleaching, we enclosed field-grown plants in cages designed to attenuate UV-B levels, but leave PAR largely unchanged (Supporting Information: Figure S3a); NaMAX2-silenced plants were enclosed in UV-B transparent cages as controls (Supporting Information: Figure S3a). Inside these UV-B opaque cages, midday UV-B fluence decreased from 220 to 30 $\mu W/cm^2$, while those of the UV-transparent cages were at 190 $\mu W/cm^2$ (Figure 5a). After 21 days

of growth, neither chlorophyll levels nor leaf colour differed significantly between plants enclosed in the two types of cages (Figure 5b, Supporting Information: Figure S3a,b). From these results, we inferred that the UV-B fluence alone was not responsible for the bleaching of irMAX2 leaves.

The Utah desert is characterised by high PAR levels, with solar maximum values of 2000 $\mu mol/m^2/s$ commonly attained at midday with values above 1000 $\mu mol/m^2/s$ for more than half of the daylight hours (Supporting Information: Figure S3c). During the 2019 field season, a majority of midday fluence values were greater than 1500 $\mu mol/m^2/s$ (Supporting Information: Figure S3d). To evaluate if these high PAR levels were responsible for the bleaching of irMAX2 plants, we enclosed plants in PAR-shade cages that reduced the midday values 10-fold to levels commonly found in the glasshouse (200 $\mu mol/m^2/s$; Figure 5c). After 21 days of growth, irMAX2 leaves fully re-greened and recovered chlorophyll a and b levels in leaves at the sensitive nodal positions (R1 to R8) compared with those of irMAX2 plants enclosed in cage-controls (Figure 5d, Supporting Information: Figure S3e). Additionally, we exposed glasshouse-grown irMAX2 plants to 1000 $\mu mol/m^2/s$ PAR levels with LED lamps for 10 days and monitored chlorophyll contents, which decreased after 2 days of high-light exposure, and by Day 6, leaves at nodes R1 to R4 were fully bleached (Supporting Information: Figure S3f,g). From these results, we inferred that exposure to high PAR levels could account for the bleaching phenotype.

To further characterise the bleaching and re-greening responses, we conducted infrared gas analyses (IRGA) of field-grown irMAX2 plants during the 2018 and 2019 field seasons. The bleached rosette and stem leaves of irMAX2 plants, but not the leaves at matched nodal positions on irD14, irKAI2 or irD14 × irKAI2 plants, had decreased photosynthetic rates (Supporting Information: Figure S4a,b). The calculated light curves of bleached irMAX2 leaves were attenuated, with lower initial slopes, light-saturated rates, and saturated photo-synthetic values; but after shade treatments, these had recovered to levels approximating those of EV leaves (Figure 5e). Ribulose-1,5-bisphosphate carboxylase/oxygenase (RuBPCase) carboxylation activi-ties, inferred from A/C_i curves calculated from field-IRGA measures, were substantially recovered after 21-days of shade treatments (Figure 5f). The nonbleached leaves of plants grown under the low-light levels (200 $\mu mol/m^2/s$) of the glasshouse had photosynthetic parameters that did not differ between EV and irMAX2 plants for: light-response curves, the maximum efficiency of PSII (Fv/Fm), the efficiency

FIGURE 2 MAX2 silencing in field-grown *Nicotiana attenuata* plants causes leaf-bleaching and impairs fitness and herbivore resistance. (a) Representative pictures of 2.5-month-old plants, and plant height, primary branching numbers of WT, irMAX2#1, irD14#2 and irKAI2#2 plants grown at Snow plot in 2018 (n = 8). (b, c) Phenotype, relative chlorophyll amount (n = 6) (b) and contents of chlorophyll a, b, chl a/b (n = 8) (c) of indicated plants grown at Lytle plot in 2019. (d) Flower numbers and capsule numbers of 2.5-month-old WT, irMAX2#1, irD14#2 and irKAI2#2 plants at 2018 field season (n = 8–10). (e) Shoot biomass flower numbers and capsule numbers of 2.5-month-old EV, two lines of irMAX2 plants at 2019 field season (n = 8–10). (f) Proportion of leaf damage of EV, irMAX2, irD14, irKAI2 and irD14 × irKAI2 plants during the 2019 field season. Each genotype includes two lines (mean ± SE, n = 46–60). Level V: leaves with 30%–40% damage, level IV: leaves with 20%–30% damage, level III: leaves with 10%–20% damage, level II: leaves with 5%–10% damage, level I: leaves with 0%–5% damage. (g) Levels of JA and JA-Ile in leaves from indicated lines without (control) or with wound treatment after 1 h (mean ± SE, n = 8). Statistical analyses were performed using Turkey's multiple comparisons test (p < 0.05) (a, c, d, e) or two-tailed Student's t. test (**p < 0.01) (g) (All values are: means ± SE).
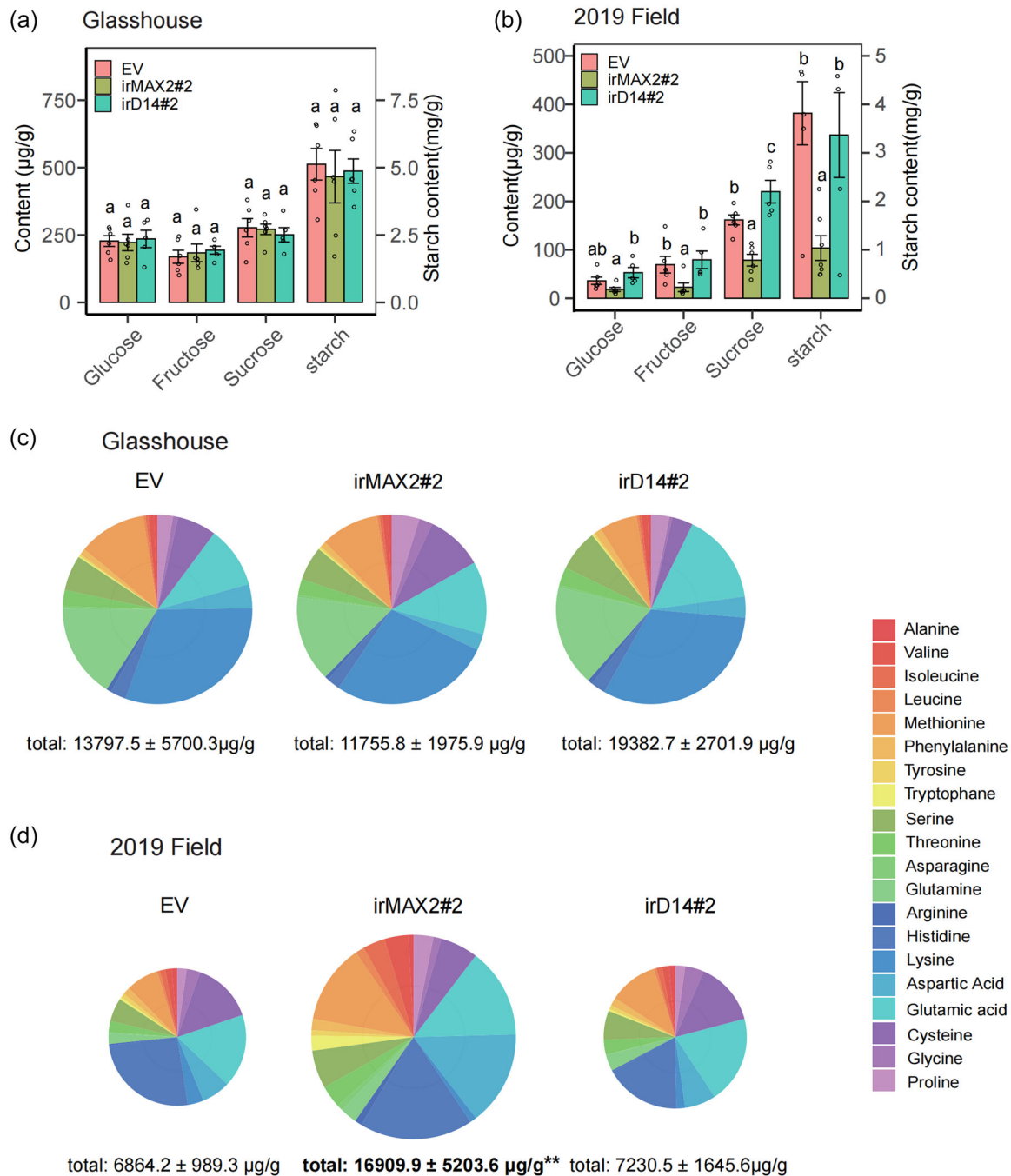
FIGURE 3 Primary metabolites were altered in irMAX2 leaves in the field. (a, b) Contents of glucose, fructose, sucrose and starch in R6-leaves of EV, irMAX2#2 and irD14#2 plants in the glasshouse (a) and during the 2019 field season (b) (mean ± SE, $n = 6$). (c, d) Proportion of amino acids in R6-leaves of EV, irMAX2#2 and irD14#2 plants grown in the glasshouse (c) and in the field in 2019 (d). Total amount of amino acids is given below the charts (mean ± SE, $n = 6$). Statistical analyses were performed using Turkey's multiple comparisons test ($p < 0.05$) (a, b) or two-tailed Student's t-test (**, $p < 0.01$) (d).

of the PS II (Fv'/Fm'), and proportion of absorbed light used for photosynthesis (PhiPSII), and non-photochemical quenching (NPQ) (Supporting Information: Figure S4c,d). From these results, we infer that high-PAR light is responsible for the bleaching phenotype and the lower photosynthetic capacity of irMAX2 plants in the field. When grown under the low-PAR light levels of the glasshouse, irMAX2 plants have normal chlorophyll levels and photosynthetic capacity.

2.6 | PAR-shading rescues antioxidant contents and ROS responses in irMAX2 leaves

High-light stress triggers a series of oxidative responses (Li et al., 2009a), in which antioxidants, such as lutein, zeaxanthin and β-carotene protect plant cells from oxidative damage caused by excessive light (Supporting Information: Figure S5a). We quantified
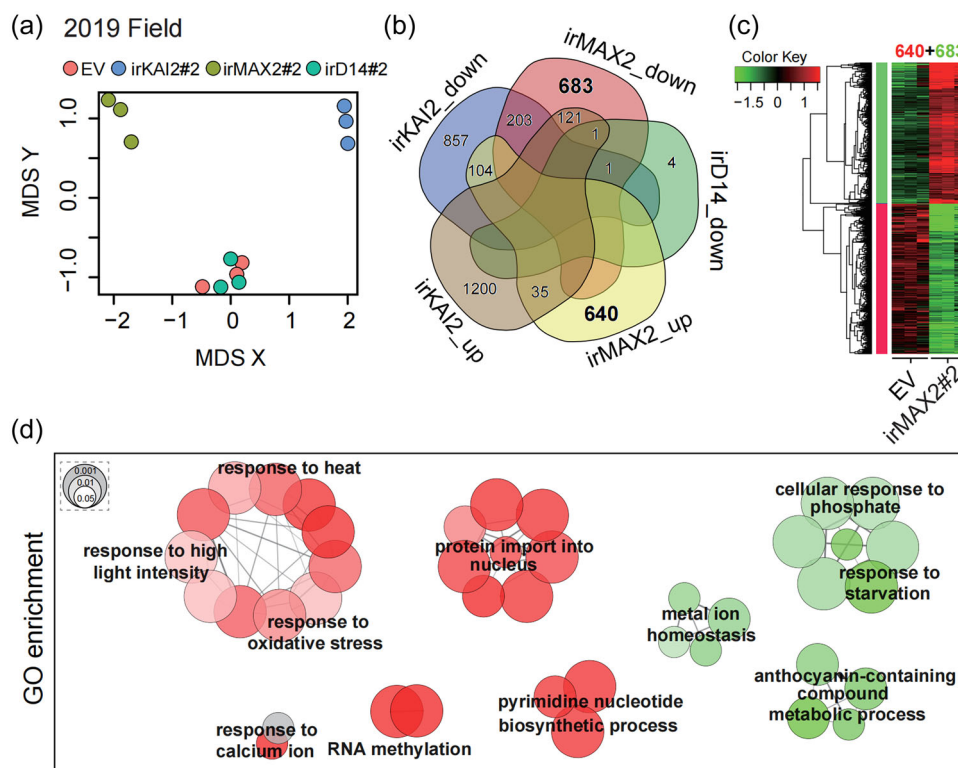
FIGURE 4 Transcriptomic analysis revealed a hypersensitive response of irMAX2 leaves to high-intensity light exposure. (a) Multidimentsional scaling (MDS) plot of the transcriptome data in EV, irKAI2#2, irMAX2#2 and irD14#2 leaves (mean ± SE, n = 3) collected during the 2019 field season. (b) Venn diagrams presenting the overlap among up- and down-regulated genes in the in EV, irKAI2#2, irMAX2#2 and irD14#2 leaves. (c) Heatmap presenting the specifically up- and down-regulated genes in the EV and irMAX2#2 leaves. (d) Gene ontology (GO) enrichment of 640 upregulated and 683 downregulated genes from (c) in the EV and irMAX2#2 leaves. The red colour presents the upregulated genes, and the blue colour presents the downregulated genes.

the levels of these three antioxidants in irMAX2 leaves. In all three field seasons, the levels of lutein were dramatically reduced in irMAX2 leaves, but not in irD14 and irKAI2 leaves; zeaxanthin levels did not differ from those of EV leaves, which were relatively low; β-carotene contents were lower than in EV leaves in 2019 field season, but higher in the 2018 and 2020 field seasons (Figure 5g, Supporting Information: Figure S5b–d). After the shade treatments in the 2019 field season, lutein contents recovered to WT levels in irMAX2 leaves, but β-carotene levels did not (Figure 5g). In glasshouse-grown plants, the levels of all three antioxidants in irMAX2 leaves did not differ from those in EV leaves (Supporting Information: Figure S5e). When these glasshouse-grown plants were exposed to high (1000 μmol/m²/s) PAR levels for 2 days, the levels of all three antioxidants increased in both lines of plants, and lutein, but not zeaxanthin and β-carotene levels, were lower in irMAX2 leaves than in EV leaves (Supporting Information: Figure S5f). These results suggest that low lutein levels contribute to the sensitivity of irMAX2 leaves to high-light stress.

Excess light is commonly associated with ROS accumulations, such as singlet oxygen, hydrogen peroxide (H_2O_2), and associated transcripts (Asada, 2006). We examined the transcript abundances of high-light responsive genes ELIP1, ELIP2, singlet oxygen responsive genes WRKY33, WRKY40-1 and WRKY40-2, and H_2O_2-catalytic and

responsive genes SOD, APX2 and ZAT10. In both the 2018 and 2019 field seasons, irMAX2 leaves had elevated levels of these marker transcripts (Figure 5h, Supporting Information: Figure S6a). After the shade treatment, the transcript levels of these genes reduced to EV-levels (Figure 5h). In response to 2 days of high-PAR exposure, the induction of transcript levels of ELIP1, ELIP2 were dramatically increased (four-fold) in irMAX2 plants (Supporting Information: Figure S6b). Surprisingly, no obvious signatures of cell-death responses were observed in irMAX2 leaves after Coomassie staining (Supporting Information: Figure S6c). From these results, we infer that the shade-reversible bleaching phenotype does not engage ROS-mediated cell-death responses and terminal senescence. However, more detailed kinetic analyses of these responses under high-PAR conditions will be required to understand the role of ROS signalling in the bleaching phenotype.

In summary, silencing NaMAX2 had opposite effects under field- and glasshouse-conditions: enhancing fitness of glasshouse-grown plants without changes in photosynthetic capacity and herbivore resistance (Figure 6a), while reducing fitness of field-grown plants by decreasing chlorophyll contents and photosynthetic capacity, and decreasing lutein contains and increasing ROS responses that are likely responsible for the observed leaf bleaching under high-light growing conditions (Figure 6b).
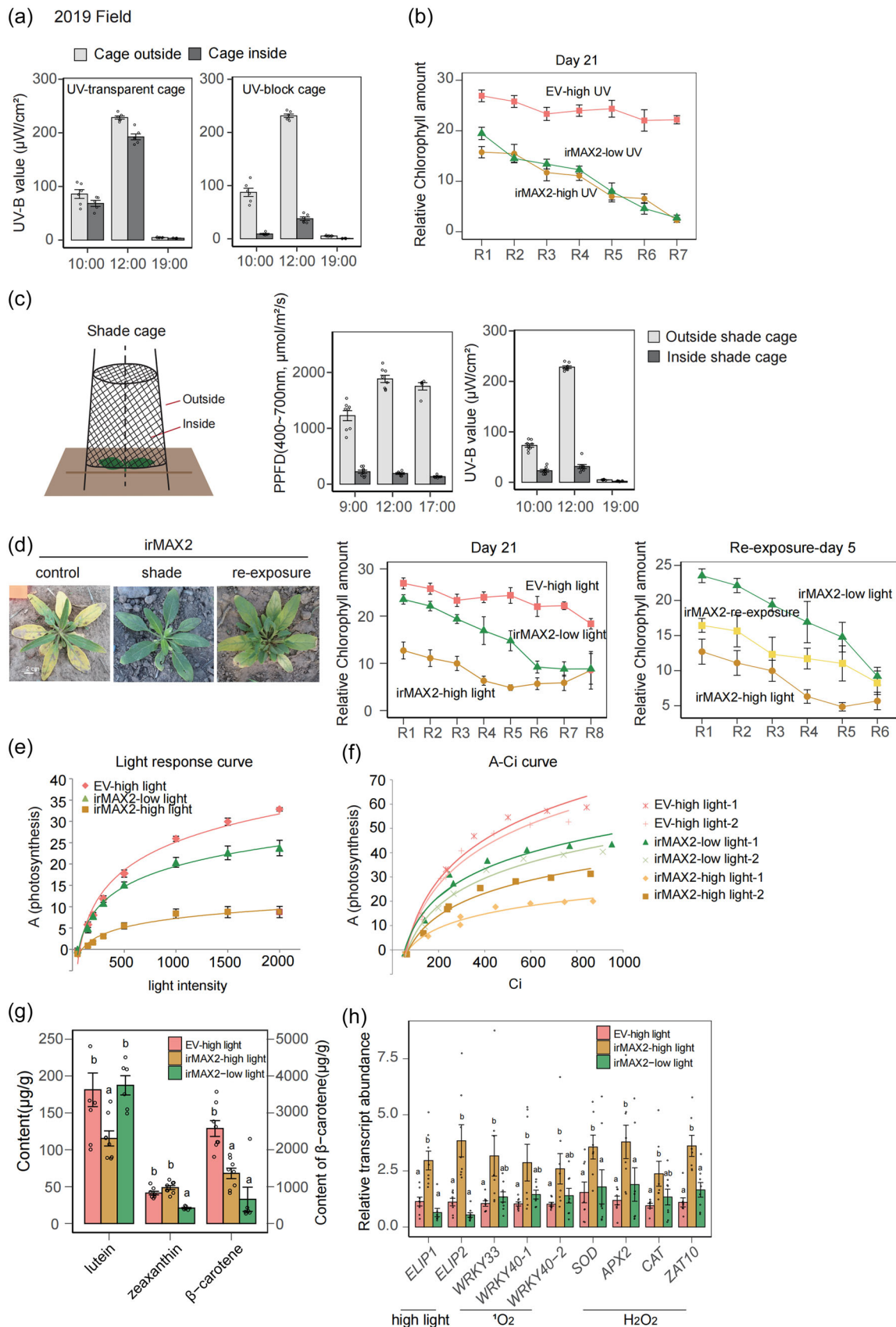
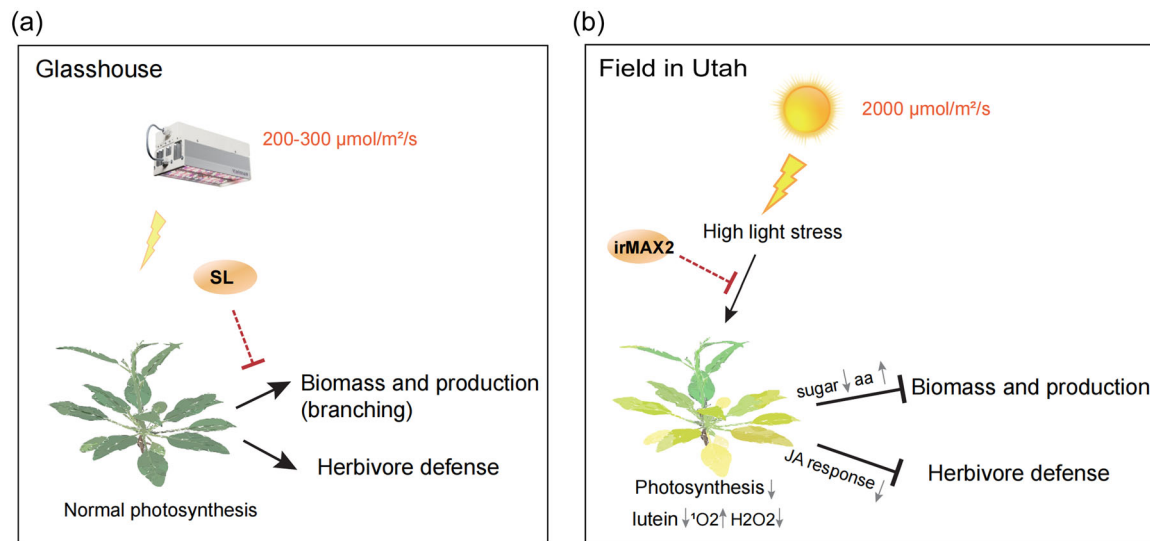**FIGURE 5** (See caption on next page).

FIGURE 6 Summary of MAX2's function in glasshouse and field. (a) When grown under the relatively low-light (200–300 μmol/m^2/s) levels that characterise glasshouse growth, irMAX2 plants develop more branches leading to increases in shoot biomass and seed production; resistance against folivores is not affected. (b) In the high-light intensities (2000 μmol/m^2/s) of the Utah desert mature leaves of irMAX2 plants bleach, decreasing photosynthesis, H_2O_2, sugars, and carotenoids levels and increasing singlet oxygen levels and protein turnover, which impairs growth, seed production, and resistance against the native folivore community.

3 | DISCUSSION

To explore the ecological function of SL and KAR signalling, we silenced key genes in these two signalling pathways in the ecological model plant, *N. attenuata*, and phenotyped these plants in field plots in a nature preserve in the plant's native habitat in the Great Basin Desert of North America. While the fitness-enhancing increases in branching of plants deficient in SL and KAR signalling are well-studied under controlled conditions (Gomez-Roldan et al., 2008; Hamiaux et al., 2012; Ishikawa et al., 2005; Umehara et al., 2008), it was not known if these phenotypes would be maintained under the extreme conditions of *N. attenuata*'s natural habitat. Surprisingly, plants silenced in *NaMAX2* expression, but not *NaD14*, *NaKAI2* or both, exhibited leaf bleaching in three consecutive years of plantings in two independently transformed lines. Off-target analysis of the ~300 bp sequences of *NaMAX2a* and *NaMAX2b* used in the RNAi

transformation constructs revealed that only *MAX2* was targeted for silencing (Supporting Information: Figure S1b). Additional field- and glasshouse-studies, suggested that this novel *MAX2* function is related to high-PAR, rather than UV-B light stress or high temperatures, independent of *MAX2*'s roles in SL and KAR signalling. However, the experiments do not rule-out possible interactions among these abiotic stressors.

Blocking UV-B from field-grown plants did not allow bleached irMAX2 plants to regreen, but decreasing PAR with the shade treatment did (Figure 5). However, this shade treatment decreased both PAR and UV-B fluences, and also likely decreased the temperatures of field-grown plants. Moreover, when glasshouse-grown (grown without UV-B) irMAX2 plants were exposed to half the solar maximum of PAR (1000 μmol/m^2/s), their bleaching was not as complete as had been observed in the field-grown plants. In addition, temperature stress is also known to influence a plant's ability to deal

FIGURE 5 Reducing photosynthetically active radiation (PAR), but not ultraviolet (UV)-B, rescues the bleaching phenotype of MAX2 silenced plants. (a) Relative UV-B fluence outside and inside of UV-block and UV-transparent cages ($n = 6$). (b) Relative chlorophyll contents of indicated leaves of EV-high UV, irMAX2-high UV (in UV-transparent cage) and irMAX2-low UV (in UV-block cage) plants ($n = 6$). (c) Schematics of the shade cage and the light intensity (PPFD) and UV-B levels outside and inside of cages. (d) Representative pictures of irMAX2-control (no-shade cage), irMAX2-shade (in shade-cage for 21 days) and irMAX2-re-exposure (in shade-cage for 21 days and cage removed for 5 days); relative chlorophyll amounts of EV-high light (no shade cage), irMAX2-high light (no shade cage) and irMAX2-low light (in shade cage) leaves with shade treatment for 21 days ($n = 8$); relative chlorophyll amounts of irMAX2-low light, irMAX2-high light and irMAX2-re-exposure leaves after removing the shade cage for 5 days ($n = 5–8$). (e) The light response curves of EV-high light, irMAX2-low light and irMAX2-high light plants ($n = 3$). (f) A–Ci curves of EV-high light, irMAX2-low light and irMAX2-high light plants, each with 2 replicates. (g) Contents of lutein, zeaxanthin, and β-carotene in leaves of EV-high light, irMAX2-high light and irMAX2-low light plants ($n = 6–8$). (h) Relative transcript abundance of high light responsive genes (*ELIP1* and *ELIP2*), H_2O_2-related genes (*SOD*, *APX2*, *CAT* and *ZAT10*) and singlet oxygen responsive genes (*WRKY33*, *WRKY40-1* and *WRKY40-2*) in leaves of EV-high light, irMAX2-high light and irMAX2-low light plants ($n = 8$). All data in this figure came from the 2019 field season. Statistical analyses were performed using Turkey's multiple comparisons test ($p < 0.05$) (g, h) (All values are means ± SE).

with high light (Demmig-Adams & Adams, 1992), and the large daily temperature fluctuations that characterise desert environments could have exacerbated the high-PAR associated leaf-bleaching of irMAX2 plants. The large literature that examined the effect of increased UV-B on crop productivity in response depletions of the ozone layer, commonly reported strong interactions between PAR and UV-B, with the deleterious effects of UV-B being exacerbated in plants grown under low PAR levels (Deckmyn & Impens, 1997; Li et al., 2009b). Clearly, addition work will be needed to examine the possible interactions of these abiotic stressors and to identify wavelengths that are responsible for the bleaching, particularly at the red and blue extremes of the PAR spectrum.

SLs and KAR signalling are both known to regulate photomorphogenesis, such as hypocotyl elongation, by mediating light signalling transduced by blue-light photoreceptor cryptochromes (CRY1 and CRY2) and red/far-red light phytochromes (phyA and phyB) (Bursch et al., 2021; Jia et al., 2014; Li et al., 2016; Nelson et al., 2010; Shen et al., 2007). Blue-light photoreceptors have recently been shown to activate chloroplast movements in response to excess light (Sakai et al., 2001; Zubik-Duda et al., 2023). However, *N. attenuata* plants silenced in the expression of NaCRY1/2, NaPhyB1/B2 and NaPhyA were planted in the field in previous field seasons without any evidence of leaf-bleaching (Oh et al., 2018; Valim et al., 2019). Moreover, transcript levels of these photoreceptor genes and *HY5* did not differ significantly among irMAX2 and irD14 and irKAI2 plants, suggesting that these aspects of light signalling were not strongly regulated in a MAX2-dependent manner in response to high PAR levels. Physiological and biochemical measures suggested that the processes that result in bleaching are slowly activated by high-light exposure.

Under low light levels (200 μmol/m^2/s) in both the field and glasshouse, irMAX2 plants produced green leaves with normal photosynthetic abilities, contents of antioxidants such as lutein, and NPQ values that reflect heat dissipation in non-photochemical quenching. When light curves are measured with glasshouse-grown irMAX2 plants, photosynthesis levels measured under short-term exposures of 2000 μmol/m^2/s PAR do not differ from those of control plants (Supporting Information: Figure S4c). However, when transferred to high-intensity light (1000 μmol/m^2/s PAR) for 2 days, concentrations of lutein and chlorophyll decreased, and transcript levels of high-light and ROS responsive genes were highly elevated in the leaves of irMAX2 plants (Supporting Information: Figures S3f,g, S5f, S6b). As lutein is the most abundant xanthophyll in higher plants which functions to stabilise antenna proteins and light harvesting, and quenching ^{3}Chl states (Jahns & Holzwarth, 2012), the impairment of lutein increases in irMAX2 leaves may affect qI, which is associated with photodamage as a component of NPQ (Leister, 2023). The high transcript levels of photo-oxidative genes in the bleached leaves of field-grown irMAX2 plants suggest intensive oxidative conditions in irMAX2 leaves. As ROS responses are known to damage chloroplast membranes and photosynthetic machinery, particularly of photosystem II, and impair photosynthetic capacity (Wang et al., 2016; Zavafer & Mancilla, 2021; Zavafer et al., 2015),

we infer that decreasing *MAX2* levels somehow decreases lutein levels, which puts PSII proteins at risk of oxidative damage and is ultimately responsible for leaf bleaching.

Field-grown irMAX2 plants have diminished photosynthetic capacity and are also more susceptible to herbivore attack and have lower wound-elicited jasmonate (JA) bursts (Figure 2f,g). We speculate that the impairment of RuBPCase carboxylation activities of irMAX2 plants (Figure 5f) might be one of the reasons for its decreased JA responses to wounding. *N. attenuata* plants silenced in the expression of RuBPCase activase by RNAi are impaired in herbivory-elicited JA-Ile levels (Mitra & Baldwin, 2008). In addition, the decreased sugar contents of irMAX2 leaves (Figure 3b) might contribute to the increased susceptibility of irMAX2 plants to folivores, as previous work revealed that larvae of the specialist herbivore, *Manduca sexta*, grow faster on low sugar-containing artificial diets and on sugar-depleted *N. attenuata* plants grown under low PAR levels (Machado et al., 2015). From these data, we infer that the greater susceptibility of irMAX2 plants to herbivore attack is directly related to the bleaching phenotype and the plants' reduced photosynthetic capacity.

There has been considerable recent interest in enhancing photosynthesis to increase crop yields by re-engineering the regulation of chlorophyll levels to minimise perceived inefficiencies in the light reactions (Leister, 2023), and even to completely re-engineer photosynthesis with the emerging synthetic biology tools (Wurtzel et al., 2019). The work described here, which points to an important and previously unrealised role for *MAX2* in protecting photosystems from high-light mediated photo-oxidative damage, underscores how much remains to be learned about how natural selection has optimised photosystems and provides another example of the value of old-fashioned field-work in understanding gene function.

4 | MATERIALS AND METHODS

4.1 | Plant material and growth

All transgenic and wild type (WT) lines were isogenic, originating from seeds collected from a plant at the DI Ranch in 1988, located 40 km north along the Beaver Dam Wash from the field station at the Lytle Ranch Preserve in the Great Basin Desert of SW USA (latitude 37.146 longitude −114.020), where all field releases were conducted. This WT genotype was self-fertilised for 31 generations to ensure homozygosity across all loci, and transformed with an established *Agrobacterium tumefaciens*–mediated transformation method (Krügel et al., 2002) using pSOL3/8/9 binary vectors harbouring a single, fully integrated inverted-repeat (ir) transformation constructs of 150–300 bp fragments of the genes targeted for silencing by RNAi. Empty vector (EV), irMAX2, irD14, irKAI2, and the hemizygous crosses (irD14 × irKAI2) were fully characterised, as described previously (Li et al., 2020). Three independent lines were used and labelled as #1–#3 for the targeted genes.

The glasshouse was located at the Max Planck Institute for Chemical Ecology in Jena, Germany. Seed germination and glasshouse growth were performed as described (Krügel et al., 2002) with a day/night cycle of 16 h (26–28°C, 200–300 µmol/m^2/s)/8 h (22–24°C). For the high-light treatment, plants were placed under high intensity LED lights in the glasshouse for 16 h (26–28°C, 900–1000 µmol/m^2/s)/8 h (22–24°C). For the high-temperature treatment, the plants were germinated under normal condition and grown for 40 days in growth rooms maintained at 14 h-days at 35°C (80 µmol/m^2/s)/10 h-nights at 18°C.

Transformed seeds were imported and released at the Lytle Ranch Preserve under the US Department of Agricultural Animal and Plant Health Inspection Service (APHIS) permit numbers 07-341-101m, 10-004-105m, 18-046-102m, 121-DGIUB96, 121-DGKKQID, 124-5923WOV, 124-5QAHAL4, 124-4VPMEMT and 124-7HQVRAG. For the 2018-2019 field seasons, seeds were germinated in hydrated 50 mm peat pellets (Jiffy 703, Always Grows, Sandusky, OH) with borax solution (Zubik-Duda et al., 2023) supplemented with soil microbes from a natural *N. attenuata* population along the Eardly road (latitude 37.101880 longitude −113.975212). The soil microbial solution (5 g/L) was stirred with a drill-operated mixer for 5 min, allowed to settle for 30 min, and used to hydrate jiffies at 1 L/100 jiffies. Germinating seedlings were maintained under shaded conditions in closed 38-quart plastic shoe-boxes with transparent lids (Walmart), floated on basins of continuously flowing water to maintain temperatures in the 15–30°C range. After 2 weeks of additional environmental adaption (in opened boxes in insect-proof mesh tents), size-matched seedlings were planted into size-matched communities of 10 plants (two from each genotype, planted in 1.5 m diameter circles). A drip irrigation system provided water to the centre of each community in a large (2 hectare) field plot that had been ploughed and harrowed the previous fall (Supporting Information: Figure S1c: at "Snow Plot" in 2018 and at "Lytle Plot" in 2019–2021). Plants were thinned to one plant per genotype/community in April, and experiments were conducted in May–June of 2018–2021.

For the 2020 and 2021 field season, smoke and GA$_3$ soaked seeds were germinated directly in the field, to allow plants to grow a natural tap-root system, unconstrained by growth initiated in Jiffy pots. A 10-cm diameter steel circular sowing template with three equally spaced 4 mm dimples, was firmly pressed into the ground 10 times around the edges of the 1.5 m diameter communities. A single seed was pipetted into each of the 3–4 mm depressions created by the sowing template and each of the single-genotype 3-seed sowings was covered by a PAR- and UV-B-transparent plastic dome lid (Solo: 9.4 × 9.4 × 2.3 cm) manufactured for 9/12/16 oz drink cups with a 1-cm circular straw slot through which a genotype-identifying label was inserted into the centre of the dome, fixing the dome firmly to the soil surface. Within a community, the 10 domes were 20 cm apart around the edge of the community equidistant from a centrally buried ring-dripper. Domes covered the seeds during germination, increasing soil temperatures and protecting recently germinated seedlings from the frequent wind storms. Germinated seedlings were thinned to a single seedling per dome between April 5 and 20; extra seedlings and soil from dimples

without a germinating seedling was removed and burned to meet regulatory requirements. Domes were removed several days later.

For shade treatments in the field, plants were covered with 40-cm tall wire cages on which black polypropylene plastic mesh with 1 cm^2 holes was fixed to reduce the total light intensity 10-fold at noon without changing the spectral composition of the light. Plants were covered during early rosette-growth and remained covered for 21 days, after which the shade-cages were removed. Plants enclosed in uncovered wire cages served as controls.

To attenuate UV-B fluence, wire cages were covered with PAR transparent, but UV-B opaque plastic (Melinex^R 506 100 micron thickness), while control cages were covered with UV-B and PAR transparent plastic wrap (Huskey clear plastic sheeting, model: RSHK403-50C-U, Grand Prairie) for 21 days, which was checked for solarisation with a hand-held UV-B metre (Solarmeter) and PAR metre (Hipoint), and replaced as needed.

For wounding treatments, leaves were damaged by rolling a fabric-pattern tracing wheel (McCloud & Baldwin, 1997) in three rows on each side of leaf and parallel to the midrib. Leaves were harvested 1 h after treatment and midribs were removed. Leaves for the analysis of phytohormones, photosynthetic pigments, amino acids, sugars, antioxidants, were harvested from standardised nodal positions (nodal positions indicated in figures), wrapped in labelled aluminium foil and immediately frozen on dry ice and shipped to the laboratory in Germany in a dry-ice shipper, where samples were stored at −80°C until analysis.

4.2 | Herbivore bioassays

Larvae of the nicotine-tolerant Lepidopteran species, *Manduca sexta* and *Spodoptera littoralis*, from in-house colonies, were used for glasshouse herbivore assays with plants that had just started the vegetative-to-reproductive transition. A single neonate *M. sexta* larva was placed on a fully expanded leaf of either EV or irMAX2 plants and allowed to move and feed freely on the entire plant. Larval biomass was weighed at the indicated days (Figure 1e). For *S. littoralis* experiments, a 1st in star larva (fed with artificial diets for 3 days after hatching) was placed on a fully expanded rosette leaf enclosed in a clip-cage, which was moved to a new leaf every 1–2 days.

Herbivore damage to field-grown plants in 2019 was visually estimated and calculated based on previously described methods (Schuman et al., 2015). When plants were in the early flowering stage (33 days-post-planting), the percentage of canopy area lost to herbivores was quantified on more than 40 plants per genotype. A majority of the damage resulted from the feeding of Noctuid cutworm larvae, adult and nymphal tree crickets and grasshoppers, and adult flea beetles.

4.3 | Photosynthesis

Photosynthetic measurements were conducted with a LI-6400XT analysis system (Li-Cor Bioscience), with a fluorometer integrated

into the leaf chamber. Measurements in the field were conducted during cloudless days between 10 AM to 14 PM. Photosynthetic rates (A) were measured with 400 μmol/m^2/s CO_2, 30°C block temperatures and 2000 μmol/m^2/s light intensity. Light response curves were conducted with the same reference CO_2 level and block temperature and at light intensity levels ranging from 0 to 2000 μmol/m^2/s. A/Ci curves were conducted with 25°C block temperatures and 2000 μmol/m^2/s light intensity at reference CO_2 levels at 7 levels from 0 to 900 μmol/m^2/s.

In the glasshouse, photosynthetic rates were measured at 400 μmol/m^2/s CO_2, 25°C block temperatures and light intensity from 0 to 2000 μmol/m^2/s. Fv/Fm, NPQ, Fv'/Fm' and PhiPSII were measured following the LICOR 6400XT manual for both dark-adapted and light-adapted measurements.

4.4 | Relative chlorophyll and leaf temperatures

Relative chlorophyll amounts and leaf temperatures were measured by a Dualex (FORCE-A) hand-held spectrophotometer of the middle lamella of fully expanded leaves of field-grown plants.

4.5 | Chlorophyll and carotenoids determination

Pulverised samples (100 mg) of leaf lamina were extracted with 600 μL methanol for chlorophyll measurements. After centrifugation, 30 μL samples of the supernatants were separated by HPLC with Acclaim C30 column (Dionex, 200 A, 3.5 μm, 4.6 × 250 mm) for pigment quantification. Pure chlorophyll a, chlorophyll b and β-carotene were used for external-standard calibrations. The mobile phases for HPLC were as follows: A: 80% methanol, B: ethyl acetate with the following gradients at a flow rate of 1 mL/min: 0 min, 80% (vol/vol) A, 20% B; 2.5 min, 77.5% A, 22.5% B; 20 min, 50% A, 50% B; 22.5 min, 50% A, 50% B; 24 min, 20% A, 80% B; 26 min, 20% A, 80% B; 31 min, 0% A, 100% B; 34 min, 0% A, 100% B; 42 min, 80% A, 20% B; 47 min, 80% A, 20% B. Chlorophyll a, chlorophyll b and β-carotene were detected at 475 nm and chlorophyll a at 440 nm, with a reference wavelength of 550 nm.

Pulverised samples (100 mg) of leaf lamina were extracted with 600 μL methanol for carotenoids measurements. After centrifugation, 20 μL samples of the supernatants separated by HPLC with Acclaim C30 column (Dionex, 200 A, 3.5 μm, 4.6 × 250 mm) to quantify carotenoids (lutein, zeaxanthin) by external standard curves with pure standards. Mobile phases for HPLC were as follows: A: methanol with ethyl acetate (1:1), B: acetonitrile, C: deionized water with 200 mM acetic acid, with the following gradients at a 1 mL/min flow rate: 0–3.6 min, 14.5% (vol/vol) A, 85% B, 0.5% C; 3.6–27 min, gradient phase to reach 34.5% A, 65% B, 0.5% C; 27–45 min, 34.5% A, 65% B, 0.5% C. Carotenoids were detected at 475 nm with a reference wavelength at 550 nm. These measurements followed the procedures described in Yang et al. (2023).

4.6 | Microarray analysis and RT-qPCR

For transcript abundance quantification, RNA was extracted from the indicated leaves using the NucleoSpin® RNA Plant (Macherey-Nagel) kits. For microarray analysis, extracted RNA from field-grown leaves was labelled and hybridised according to the protocol of the Quick Amp labelling kit (Agilent, http://www.agilent.com/home). For hybridisations, Agilent single-colour technology arrays (60 k) were used. Raw intensity data were normalised with the quantile method, and the probes with low expression levels were discarded after log$_2$ transformation. Differentially expressed probes were filtered after pair-wise comparisons (|Fold Change| ≥2, FDR ≤ 0.05).

For RT-qPCR, cDNA was prepared by using the PrimeScript RT-qPCR Kit (TaKaRa). RT-qPCR was performed on a Mx3005P qPCR machine using a SYBR Green reaction mix (Eurogentec, qPCR kit SYBR Green I No ROX). For all RT-qPCR analysis, the *N. attenuata* IF-5a housekeeping gene was used as an internal reference. Primer sequences were listed in the Supporting Information Table S1.

4.7 | Sugar determination

To determine sugar levels, 100 mg of pulverised R6 (see Figure 1b for leaf position determinations) leaf samples of leaf lamina were extracted with 800 μL extraction buffer (0.2 N formic acid in 80% MeOH). After centrifugation, extracts were diluted 200-fold with 500 pmol/μL sorbitol (standard) for HPLC-MS analysis following the procedures described in Schäfer et al. (2016). The analysis was performed on a Bruker Elite EvoQ triple-quadrupole MS equipped with a heated electrospray ionisation (HESI) ion source.

4.8 | Amino acids determination

To determine amino acid levels, 100 mg pulverised leaf samples of leaf lamina were extracted with 800 μL extraction buffer (0.2 N formic acid in 80% MeOH). After centrifugation, extracts were diluted 50-fold with 1 ng/g amino acid standard mix for HPLC-MS analysis following the procedures in Schäfer et al. (2016). The analysis was performed on a Bruker Elite EvoQ triple-quadrupole MS equipped with a HESI ion source.

4.9 | Jasmonate measurements

To determine jasmonates (JA and JA-Ile) levels, 100 mg of pulverised leaf samples of leaf lamina were extracted with 800 μL extraction buffer (0.2 N formic acid in 80% MeOH with isotopically labelled JA internal standards). After centrifugation, extracts were used for HPLC-MS analysis following the procedures described in Schäfer et al. (2016). The analysis was performed on a Bruker Elite EvoQ triple-quadrupole MS equipped with a HESI ion source.

4.10 | Nutrient determination

The leaves of transgenic plants (five plants per each line) were harvested in the 2019 field season at the end of the experiment and subjected to carbon and nitrogen elemental analysis. Briefly, oven dried leaves were pulverised using a sample mill to a fine powder. Total C and N contents (mg/g) were analysed with Vario EL CNS analyser (Elementary Analyse System GmbH). For other nutritional elements measurements, finely powdered leaf samples were dissolved in 65% nitric acid (HNO_3), and the concentrations (mg/g) were determined by inductively coupled plasma atomic emission spectrometry (ICP-AES, Spectro) (Jenkinson & Powlson, 1976; Vance et al., 1987).

CONFLICT OF INTEREST STATEMENT

The authors declare no conflict of interest.

DATA AVAILABILITY STATEMENT

The data that support the findings of this study are available from the corresponding author upon reasonable request.

ORCID

Suhua Li http://orcid.org/0000-0001-6825-6203
Jianbei Huang http://orcid.org/0000-0001-5286-5645
Ian T. Baldwin http://orcid.org/0000-0001-5371-2974

REFERENCES

Akiyama, K., Matsuzaki, K. & Hayashi, H. (2005) Plant sesquiterpenes induce hyphal branching in arbuscular mycorrhizal fungi. *Nature*, 435, 824–827. Available from: https://doi.org/10.1038/nature03608

Asada, K. (2006) Production and scavenging of reactive oxygen species in chloroplasts and their functions. *Plant Physiology*, 141, 391–396. Available from: https://doi.org/10.1104/pp.106.082040

Bursch, K., Niemann, E.T., Nelson, D.C. & Johansson, H. (2021) Karrikins control seedling photomorphogenesis and anthocyanin biosynthesis through a HY5-BBX transcriptional module. *The Plant Journal*, 107, 1346–1362. Available from: https://doi.org/10.1111/tpj.15383

Chi, C., Xu, X., Wang, M., Zhang, H., Fang, P., Zhou, J., et al. (2021) Strigolactones positively regulate abscisic acid-dependent heat and cold tolerance in tomato. *Horticulture Research*, 8, 237. Available from: https://doi.org/10.1038/s41438-021-00668-y

Cook, C.E., Whichard, L.P., Turner, B., Wall, M.E. & Egley, G.H. (1966) Germination of witchweed (*Striga lutea* Lour.)—isolation and properties of a potent stimulant. *Science*, 154, 1189–1190. Available from: https://doi.org/10.1126/science.154.3753.1189

Deckmyn, G. & Impens, I. (1997) The ratio UV-B photosynthetically active radiation (PAR) determines the sensitivity of rye to increased UV-B radiation. *Environmental and Experimental Botany*, 37, 3–12. Available from: https://doi.org/10.1016/S0098-8472(96)01044-1

Demmig-Adams, B. & Adams, III, W.W. (1992) Photoprotection and other responses of plants to high light stress. *Annual Review of Plant Physiology and Plant Molecular Biology*, 43, 599–626.

Gomez-Roldan, V., Fermas, S., Brewer, P.B., Puech-Pagès, V., Dun, E.A., Pillot, J.P., et al. (2008) Strigolactone inhibition of shoot branching. *Nature*, 455, 189–194. Available from: https://doi.org/10.1038/nature07271

Guan, J.C., Li, C., Flint-Garcia, S., Suzuki, M., Wu, S., Saunders, J.W., et al. (2022) Maize domestication phenotypes reveal strigolactone networks coordinating grain size evolution with kernel-bearing cupule architecture. *The Plant Cell*, 35, 1013–1037. Available from: https://doi.org/10.1093/plcell/koac370

Ha, C.V., Leyva-González, M.A., Osakabe, Y., Tran, U.T., Nishiyama, R., Watanabe, Y., et al. (2014) Positive regulatory role of strigolactone in plant responses to drought and salt stress. *Proceedings of the National Academy of Sciences United States of America*, 111, 851–856. Available from: https://doi.org/10.1073/pnas.1322135111

Hamiaux, C., Drummond, R.S.M., Janssen, B.J., Ledger, S.E., Cooney, J.M., Newcomb, R.D. et al. (2012) DAD2 is an α/β hydrolase likely to be involved in the perception of the plant branching hormone, strigolactone. *Current Biology*, 22, 2032–2036. Available from: https://doi.org/10.1016/j.cub.2012.08.007

Ishikawa, S., Maekawa, M., Arite, T., Onishi, K., Takamure, I. & Kyozuka, J. (2005) Suppression of tiller bud activity in tillering dwarf mutants of rice. *Plant and Cell Physiology*, 46, 79–86. Available from: https://doi.org/10.1093/pcp/pci022

Jahns, P. & Holzwarth, A.R. (2012) The role of the xanthophyll cycle and of lutein in photoprotection of photosystem II. *Biochimica et Biophysica Acta (BBA) - Bioenergetics*, 1817, 182–193. Available from: https://doi.org/10.1016/j.bbabio.2011.04.012

Janik, E., Bednarska, J., Zubik, M., Puzio, M., Luchowski, R., Grudzinski, W., et al. (2013) Molecular architecture of plant thylakoids under physiological and light stress conditions: a study of lipid-light-harvesting complex II model membranes. *The Plant Cell*, 25, 2155–2170. Available from: https://doi.org/10.1105/tpc.113.113076

Jenkinson, D.S. & Powlson, D.S. (1976) The effects of biocidal treatments on metabolism in soil—V. *Soil Biology and Biochemistry*, 8, 209–213. Available from: https://doi.org/10.1016/0038-0717(76)90005-5

Jia, K.P., Luo, Q., He, S.B., Lu, X.D. & Yang, H.Q. (2014) Strigolactone-regulated hypocotyl elongation is dependent on cryptochrome and phytochrome signaling pathways in Arabidopsis. *Molecular Plant*, 7, 528–540. Available from: https://doi.org/10.1093/mp/sst093

Kallenbach, M., Bonaventure, G., Gilardoni, P.A., Wissgott, A. & Baldwin, I.T. (2012) Empoasca leafhoppers attack wild tobacco plants in a jasmonate-dependent manner and identify jasmonate mutants in natural populations. *Proceedings of the National Academy of Sciences*, 109, 1548–1557. Available from: https://doi.org/10.1073/pnas.1200363109

Kasahara, M., Kagawa, T., Oikawa, K., Suetsugu, N., Miyao, M. & Wada, M. (2002) Chloroplast avoidance movement reduces photodamage in plants. *Nature*, 420, 829–832. Available from: https://doi.org/10.1038/nature01213

Krügel, T., Lim, M., Gase, K., Halitschke, R. & Baldwin, I.T. (2002) Agrobacterium-mediated transformation of *Nicotiana attenuata*, a model ecological expression system. *Chemoecology*, 12, 177–183.

Lahari, Z., Ullah, C., Kyndt, T., Gershenzon, J. & Gheysen, G. (2019) Strigolactones enhance root-knot nematode (*Meloidogyne graminicola*) infection in rice by antagonizing the jasmonate pathway. *New Phytologist*, 224, 454–465. Available from: https://doi.org/10.1111/nph.15953

Leister, D. (2023) Enhancing the light reactions of photosynthesis: strategies, controversies, and perspectives. *Molecular Plant*, 16, 4–22. Available from: https://doi.org/10.1016/j.molp.2022.08.005

Li, S., Chen, L., Li, Y., Yao, R., Wang, F., Yang, M., et al. (2016) Effect of GR24 stereoisomers on plant development in Arabidopsis. *Molecular Plant*, 9, 1432–1435. Available from: https://doi.org/10.1016/j.molp.2016.06.012

Li, S., Joo, Y., Cao, D., Li, R., Lee, G. & Halitschke, R. et al. (2020) Strigolactone signaling regulates specialized metabolism in tobacco stems and interactions with stem-feeding herbivores. *PLoS Biology*, 18, e3000830. Available from. https://doi.org/10.1371/journal.pbio.3000830

Li, W., Nguyen, K.H., Chu, H.D., Ha, C.V., Watanabe, Y., Osakabe, Y., et al. (2017) The karrikin receptor KAI2 promotes drought resistance in *Arabidopsis thaliana*. *PLoS Genetics*, 13. e1007076. Available from: https://doi.org/10.1371/journal.pgen.1007076

Li, Z., Wakao, S., Fischer, B.B. & Niyogi, K.K. (2009a) Sensing and responding to excess light. *Annual review of plant biology*, 60, 239–260. Available from: https://doi.org/10.1146/annurev.arplant.58.032806.103844

Li, Z., Wakao, S., Fischer, B.B. & Niyogi, K.K. (2009b) Sensing and responding to excess light. *Annual review of plant biology*, 60, 239–260. Available from: https://doi.org/10.1146/annurev.arplant.58.032806.103844

Machado, R.A.R., Arce, C.C.M., Ferrieri, A.P., Baldwin, I.T. & Erb, M. (2015) Jasmonate-dependent depletion of soluble sugars compromises plant resistance to *Manduca sexta*. *New Phytologist*, 207, 91–105. Available from: https://doi.org/10.1111/nph.13337

McCloud, E.S. & Baldwin, I.T. (1997) Herbivory and caterpillar regurgitants amplify the wound-induced increases in jasmonic acid but not nicotine in *Nicotiana sylvestris*. *Planta*, 203, 430–435. Available from: https://doi.org/10.1007/s004250050210

Mitra, S. & Baldwin, I.T. (2008) Independently silencing two photosynthetic proteins in *Nicotiana attenuata* has different effects on herbivore resistance. *Plant Physiology*, 148, 1128–1138. Available from: https://doi.org/10.1104/pp.108.124354

Nakamura, H., Xue, Y.L., Miyakawa, T., Hou, F., Qin, H.M., Fukui, K., et al. (2013) Molecular mechanism of strigolactone perception by DWARF14. *Nature Communications*, 4, 2613.

Nelson, D.C., Flematti, G.R., Riseborough, J.A., Ghisalberti, E.L., Dixon, K.W. & Smith, S.M. (2010) Karrikins enhance light responses during germination and seedling development in *Arabidopsis thaliana*. *Proceedings of the National Academy of Sciences United States of America*, 107, 7095–7100. Available from: https://doi.org/10.1073/pnas.0911635107

Nelson, D.C., Scaffidi, A., Dun, E.A., Waters, M.T., Flematti, G.R., Dixon, K.W., et al. (2011) F-box protein MAX2 has dual roles in karrikin and strigolactone signaling in *Arabidopsis thaliana*. *Proceedings of the National Academy of Sciences United States of America*, 108, 8897–8902. Available from: https://doi.org/10.1073/pnas.1100987108

Oh, Y., Fragoso, V., Guzzonato, F., Kim, S.G., Park, C.M. & Baldwin, I.T. (2018) Root-expressed phytochromes B1 and B2, but not PhyA and Cry2, regulate shoot growth in nature. *Plant, Cell & Environment*, 41, 2577–2588. Available from: https://doi.org/10.1111/pce.13341

Poorter, H., Fiorani, F., Pieruschka, R., Wojciechowski, T., van der Putten, W.H., Kleyer, M., et al. (2016) Pampered inside, pestered outside? differences and similarities between plants growing in controlled conditions and in the field. *New Phytologist*, 212, 838–855. Available from: https://doi.org/10.1111/nph.14243

Ramel, F., Birtic, S., Cuiné, S., Triantaphylidès, C., Ravanat, J.L. & Havaux, M. (2012) Chemical quenching of singlet oxygen by carotenoids in plants. *Plant Physiology*, 158, 1267–1278. Available from: https://doi.org/10.1104/pp.111.182394

Sakai, T., Kagawa, T., Kasahara, M., Swartz, T.E., Christie, J.M., Briggs, W.R., et al. (2001) Arabidopsis nph1 and npl1: blue light receptors that mediate both phototropism and chloroplast relocation. *Proceedings of the National Academy of Sciences United States of America*, 98, 6969–6974. Available from: https://doi.org/10.1073/pnas.101137598

Sánchez-Moreiras, A.M. & Reigosa, M.J. (2018) *Advances in plant ecophysiology techniques*, 1st ed. Springer International Publishing: Springer, pp. 153–175.

Schäfer, M., Brütting, C., Baldwin, I.T. & Kallenbach, M. (2016) High-throughput quantification of more than 100 primary- and secondary-metabolites, and phytohormones by a single solid-phase extraction based sample preparation with analysis by UHPLC-HESI-MS/MS. *Plant Methods*, 12, 30. Available from: https://doi.org/10.1186/s13007-016-0130-x

Schuman, M.C., Allmann, S. & Baldwin, I.T. (2015) Plant defense phenotypes determine the consequences of volatile emission for individuals and neighbors. *eLife*, 4:e04490.

Schuman, M.C. & Baldwin, I.T. (2018) Field studies reveal functions of chemical mediators in plant interactions. *Chemical Society Reviews*, 47, 5338–5353. Available from: https://doi.org/10.1039/c7cs00749c

Shen, H., Luong, P. & Huq, E. (2007) The F-box protein MAX2 functions as a positive regulator of photomorphogenesis in Arabidopsis. *Plant Physiology*, 145, 1471–1483. Available from: https://doi.org/10.1104/pp.107.107227

Smith, S.M. & Li, J. (2014) Signalling and responses to strigolactones and karrikins. *Current Opinion in Plant Biology*, 21, 23–29. Available from: https://doi.org/10.1016/j.pbi.2014.06.003

Sofo, A., Scopa, A., Nuzzaci, M. & Vitti, A. (2015) Ascorbate peroxidase and catalase activities and their genetic regulation in plants subjected to drought and salinity stresses. *International Journal of Molecular Sciences*, 16, 13561–13578. Available from: https://doi.org/10.3390/ijms160613561

Sztatelman, O., Waloszek, A., Katarzyna Banaś, A. & Gabryś, H. (2010) Photoprotective function of chloroplast avoidance movement: in vivo chlorophyll fluorescence study. *Journal of Plant Physiology*, 167, 709–716. Available from: https://doi.org/10.1016/j.jplph.2009.12.015

Umehara, M., Hanada, A., Yoshida, S., Akiyama, K., Arite, T., Takeda-Kamiya, N., et al. (2008) Inhibition of shoot branching by new terpenoid plant hormones. *Nature*, 455, 195–200. Available from: https://doi.org/10.1038/nature07272

Valim, H.F., McGale, E., Yon, F., Halitschke, R., Fragoso, V., Schuman, M.C. et al. (2019) The clock gene TOC1 in shoots, not roots, determines fitness of *Nicotiana attenuata* under drought. *Plant Physiology*, 181, 305–318. Available from: https://doi.org/10.1104/pp.19.00286

Vance, E.D., Brookes, P.C. & Jenkinson, D.S. (1987) An extraction method for measuring soil microbial biomass C. *Soil Biology and Biochemistry*, 19, 703–707. Available from: https://doi.org/10.1016/0038-0717(87)90052-6

Wang, F., Han, T., Song, Q., Ye, W., Song, X., Chu, J., et al. (2020) The rice circadian clock regulates tiller growth and panicle development through strigolactone signaling and sugar sensing. *The Plant Cell*, 32, 3124–3138. Available from: https://doi.org/10.1105/tpc.20.00289

Wang, L., Kim, C., Xu, X., Piskurewicz, U., Dogra, V., Singh, S., et al. (2016) Singlet oxygen- and EXECUTER1-mediated signaling is initiated in grana margins and depends on the protease FtsH2. *Proceedings of the National Academy of Sciences United States of America*, 113, 3792–3800. Available from: https://doi.org/10.1073/pnas.1603562113

Waters, M.T., Nelson, D.C., Scaffidi, A., Flematti, G.R., Sun, Y.K., Dixon, K.W. et al. (2012a) Specialisation within the DWARF14 protein family confers distinct responses to karrikins and

strigolactones in Arabidopsis. *Development*, 139, 1285–1295. Available from: https://doi.org/10.1242/dev.074567

Waters, M.T., Nelson, D.C., Scaffidi, A., Flematti, G.R., Sun, Y.K., Dixon, K.W. et al. (2012b) Specialisation within the DWARF14 protein family confers distinct responses to karrikins and strigolactones in Arabidopsis. *Development*, 139, 1285–1295. Available from: https://doi.org/10.1242/dev.074567

Wurtzel, E.T., Vickers, C.E., Hanson, A.D., Millar, A.H., Cooper, M., Voss-Fels, K.P., et al. (2019) Revolutionizing agriculture with synthetic biology. *Nature Plants*, 5, 1207–1210. Available from: https://doi.org/10.1038/s41477-019-0539-0

Xu, X., Fang, P., Zhang, H., Chi, C., Song, L., Xia, X., et al. (2019) Strigolactones positively regulate defense against root-knot nematodes in tomato. *Journal of Experimental Botany*, 70, 1325–1337. Available from: https://doi.org/10.1093/jxb/ery439

Yang, C., Bai, Y., Halitschke, R., Gase, K., Baldwin, G. & Baldwin, I.T. (2023) Exploring the metabolic basis of growth/defense tradeoffs in complex environments with *Nicotiana attenuata* plants co-silenced in NaMYC2a/b expression. *New Phytologist*, 238, 349–366. Available from: https://doi.org/10.1111/nph.18732

Yao, R., Ming, Z., Yan, L., Li, S., Wang, F., Ma, S., et al. (2016) DWARF14 is a non-canonical hormone receptor for strigolactone. *Nature*, 536, 469–473. Available from: https://doi.org/10.1038/nature19073

Zavafer, A., Cheah, M.H., Hillier, W., Chow, W.S. & Takahashi, S. (2015) Photodamage to the oxygen evolving complex of photosystem II by visible light. *Scientific Reports*, 5. 16363. Available from: https://doi.org/10.1038/srep16363

Zavafer, A. & Mancilla, C. (2021) Concepts of photochemical damage of photosystem II. *Journal of Photochemistry and Photobiology, C:*

Photochemistry Reviews, 47, 100421. Available from: https://doi.org/10.1016/j.jphotochemrev.2021.100421

Zhao, J., Wang, T., Wang, M., Liu, Y., Yuan, S., Gao, Y., et al. (2014) DWARF3 participates in an SCF complex and associates with DWARF14 to suppress rice shoot branching. *Plant and Cell Physiology*, 55, 1096–1109. Available from: https://doi.org/10.1093/pcp/pcu045

Zubik-Duda, M., Luchowski, R., Maksim, M., Nosalewicz, A., Zgłobicki, P., Banaś, A.K., et al. (2023) The photoprotective dilemma of a chloroplast: to avoid high light or to quench the fire? *The Plant Journal*, 115, 7–17. Available from: https://doi.org/10.1111/tpj.16221

Zurzycki, J. (2017) Chloroplasts arrangement as a factor in photosynthesis. *Acta Societatis Botanicorum Poloniae*, 24, 27–63.

SUPPORTING INFORMATION

Additional supporting information can be found online in the Supporting Information section at the end of this article.

How to cite this article: Li, S., Baldwin, G., Yang, C., Lu, R., Meng, S., Huang, J. et al. (2024) Field-work reveals a novel function for MAX2 in a native tobacco's high-light adaptions. *Plant, Cell & Environment*, 47, 230–245. https://doi.org/10.1111/pce.14728